ARMA/USRMS 06-1159

High-Resolution Seismic Monitoring at Mt. Keith Open Pit Mine

Sweby, G.J.
Australian Centre for Geomechanics, Perth, WA, Australia
Trifu, C-I.
Engineering Seismology Group, Kingston, Ontario, Canada
Goodchild, D.J. and Morris, L.D.
BHP Billiton (Nickel West), Perth, WA, Australia

ABSTRACT: A system configuration is designed to monitor microseismicity at trial sites located at Mt. Keith open pit mine in Western Australia. Array sensitivity allows for the location of events down to magnitude -1.6 with 5m accuracy. A total of 270 seismic events with magnitudes between -1.6 and -0.6 are recorded during 6 months of monitoring at the first of three trial sites. It is outlined that 90% of recorded seismicity is characterized by E_S/E_P ratios less than 5.5, suggesting that the predominant failure mechanism is crushing or dilatational behaviour. Trial monitoring results are further used in defining final array configuration.

1. INTRODUCTION

In Western Australia, the open pit mining industry is operating at increasing depths and there are current plans for developing a number of deep pits. It is well documented that this region has an anomalously high horizontal to vertical stress ratio of about 2.5 [1]. It is thus anticipated that new geotechnical problems caused by high in-situ stress will develop in future deep open pit mines. Some of these problems will manifest in the pit floor while others are likely to occur in the walls. Failure mechanisms driven by a combination of shear on pre-existing structures and stress induced fracturing, presently uncommon in the region, will likely become a major risk in future deep open pits. Although evidence of such failure mechanisms has already been observed in some of the current deeper pits, there is much to be learned about this new risk. Since classical design approaches do not account for such failure mechanisms, future deep pits may be sub-optimally designed, leading to potential wall-scale failures and unforeseen business risk.

In order to mitigate the above risks, it was proposed to apply microseismic monitoring for understanding the deep-seated failure processes that affect slopes in high- or over-stressed mining environments. As such, a project on high-resolution monitoring of mining induced seismicity associated with open pit mining has been underway in Western Australia over the past two years. BHP Billiton has provided three trial sites at Mt. Keith Nickel Operation, for the temporary installation of six-channel uniaxial geophone arrays. These three sites are to be monitored for a period of several months to determine which site will provide the maximum benefit for both the project and the mine's needs. The selected trial site will be then expanded to a larger, final array design for permanent monitoring.

This study summarizes the work carried out at the first trial site. First, it presents the microseismic system configuration, along with the sensor array design. Since geophones and accelerometers were installed in tandem at the same locations, this allows for their comparison. The results obtained over a six-month monitoring are then reported, as well as the anticipated system expansion.

2. SITE LOCATION AND OBJECTIVES

BHP Billiton's Mt. Keith Nickel Operation is located some 700 km NE of Perth in central

Western Australia (Fig. 1). Geologically, Mt. Keith orebody falls within the komatiite-hosted nickel deposits of the Yilgarn Craton formed about 2.7 billion years ago.

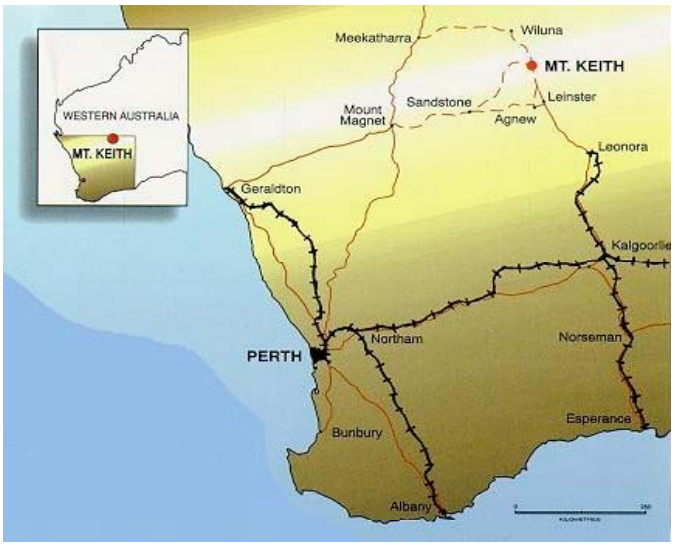

Fig. 1. Mt. Keith Nickel Operation in Western Australia.

Three trial sensor arrays have been installed to date around the northern half of the pit to monitor the seismic activity associated with current mining areas (Fig. 2). Site 319 represents the first trial site, for which the results of a six-month monitoring are presented in the following sections.

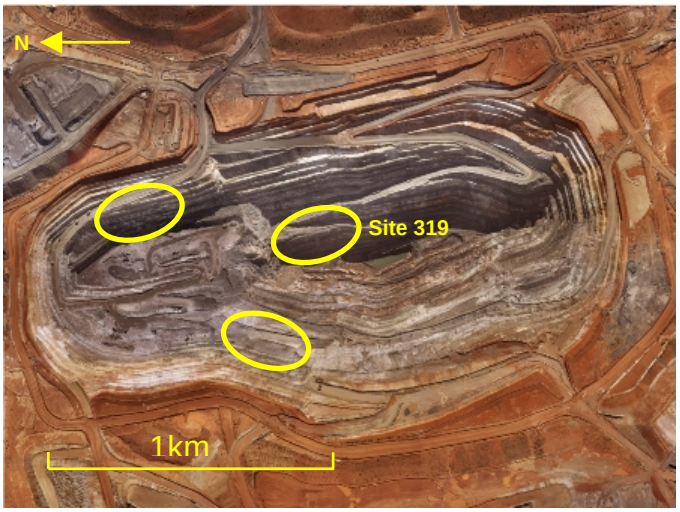

Fig. 2. Location of trial seismic arrays.

The main objective during the trial period is to determine which of the three areas is the most active and would therefore provide the most useful information to both the project and the sponsor. Consequently, the main task during the trial phase is to determine the level of seismic activity (number of events) in each area. An event location accuracy of 5 m and a magnitude sensitivity of -2 are targeted.

Secondary tasks are to experiment with different array designs, investigate the benefits of using geophones versus accelerometers, and identify and eliminate any potential problems associated with the installation and operation of monitoring hardware.

3. SEISMIC SYSTEM CONFIGURATION

The microseismic system is based on ESG Paladin recorders. This recorder offers six-channel, 24-bit resolution continuous data acquisition at a sampling frequency of up to 10 kHz and Ethernet TCP/IP telemetry. A remote station consists of the seismic recorder, GPS time receiver, Ethernet antenna, and solar-powered electrical supply (Fig. 3). Stations, conveniently placed on skids for easy installation and redeployment, communicate via wireless networking, by a series of repeaters, to a central receiving station located in the mine offices.

Fig. 3. Remote seismic station setup.

To record microseismic events with magnitudes down to -2, piezoelectric accelerometers with a frequency bandwidth of 50 to 5,000 Hz and a sensitivity of 30 V/g and 15 Hz omni-directional geophones with a frequency range of 6 to 1,000 Hz and a sensitivity of 43.3 V/m/s are selected. Continuous data acquisition is carried out at 2.5 kHz sampling. Event location to within 5 m accuracy requires that inter-sensor distance be kept less than 100 m.

Each trial array is designed to incorporate six uniaxial sensors installed in three percussion boreholes drilled inclined from nearby surface

locations, two sensors per hole. At the first trial site, both accelerometers and geophones are installed at the very same locations for comparison purposes. The borehole design for the first trial array (Site 319) is shown in Fig. 4.

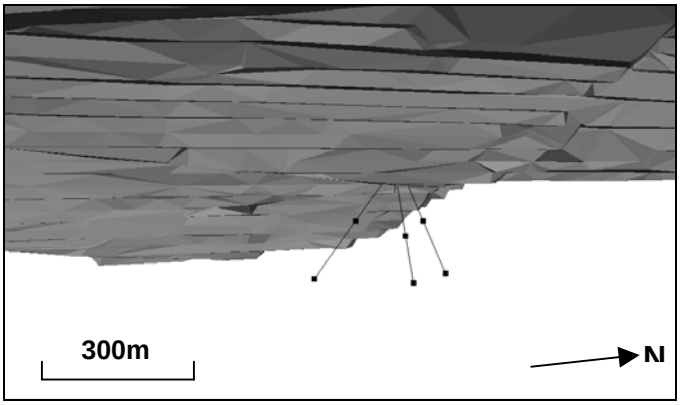

Fig. 4. Sensor array design for Site 319.

An array design spreadsheet procedure was developed to assist with comparative array design evaluation based on location accuracy. Event location error is estimated as the square root of the sum of squared standard deviations of spatial coordinates. Error contours corresponding to events within or close to the array are presented in Fig. 5.

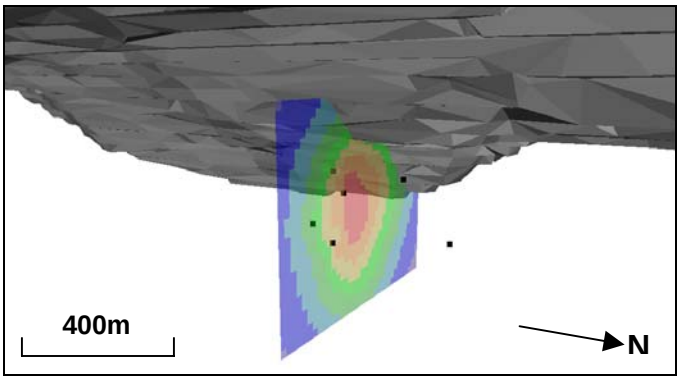

Fig. 5. Predicted location errors.

As expected, the lowest location errors are obtained for events occurring in the center of the array, with accuracy decreasing towards extremities. The shape of location errorspace within monitored volume can be visualized by cross-section iso-surfaces in three-dimensions. A circular errorspace pattern indicates the presence of only one inversion minimum and conditions for reliable location results.

4. GEOPHONES VS. ACCELEROMETERS

As indicated earlier, uniaxial geophones and accelerometers were installed at identical locations at Site 319 (Fig. 6). After three months of monitoring, the merits of each sensor type are concluded upon based on a comparative analysis. The results obtained indicate that the geophones are more sensitive (have a higher effective response). Thus, they detect more cultural noise generated by mining activities. They also have the potential to detect to record large magnitude events due to their lower frequency limit.

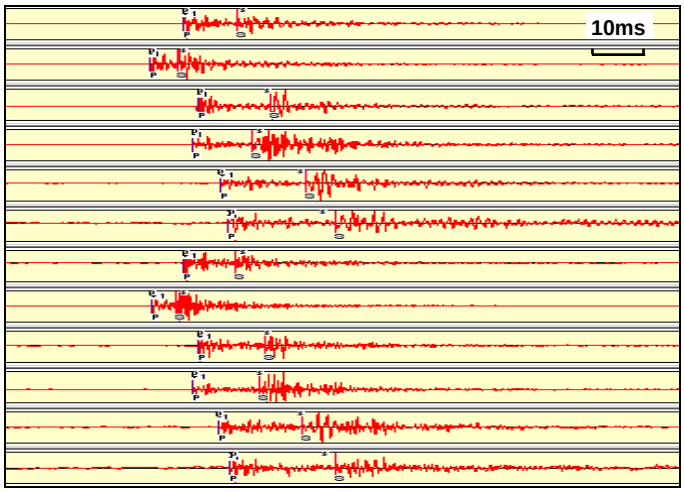

Fig. 6. Example of event recordings from geophones (channels 1-6) and accelerometers (channels 7-12).

The analysis also concludes that source parameters estimates for events with magnitudes less then approximately -1 are less reliable as determined from geophone recordings. For such an event, a comparison of the observed S-wave displacement amplitude spectra fit to the ω^{-2} model from a geophone and an accelerometer placed at the same location is shown in Fig. 7. Corner frequency estimates are around 500 Hz. Meanwhile, the smaller variance of spectral derived parameters from accelerometers is apparent.

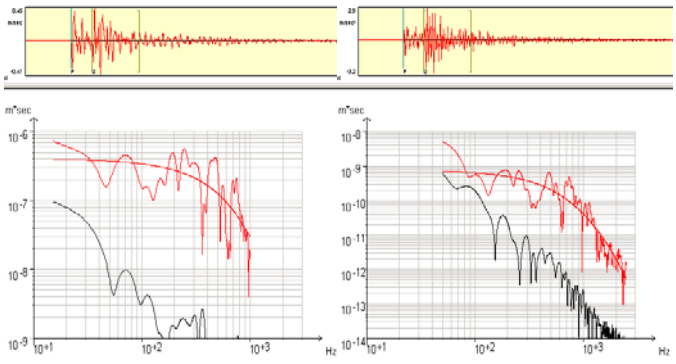

Fig. 7. Comparison of S-wave displacement amplitude spectra derived from geophone (left) and accelerometer (right) recordings (channels 2 and 8 in Fig. 6, respectively). Noise spectra, of lower amplitudes, are calculated for a time window of equal length to the signal, prior to the arrival of the P-wave.

5. RESULTS

A total of 270 seismic events were recorded from March till September 2005. Event locations employ both P and S-wave arrivals. Moment magnitudes are estimated from

$$M = 2/3 \log M_0 - 6.0, \quad (1)$$

where M_0 is the seismic moment in Nm,

$$M_0 = 4\pi\rho c^3 R\Omega_{0c} / F_c, \; \Omega_{0c}^2 = 4S_{D2c}^{3/2} S_{V2c}^{-1/2}, \quad (2)$$

with R the source-sensor distance, ρ the density of seismic source material, c the P or S-wave velocity, F_c the source average radiation pattern $(F_P = 0.52, F_S = 0.63)$, S_{D2c}, S_{V2c} the integrals of squared displacement and velocity, respectively, calculated in the time domain for each wavetype [2]. Fig. 8 shows event magnitude occurrence over monitoring period, with the slope of the cumulative number of events giving an indication of the activity rate. A significant slope increase occurred in May, coinciding with a period of heavy rainfall on site.

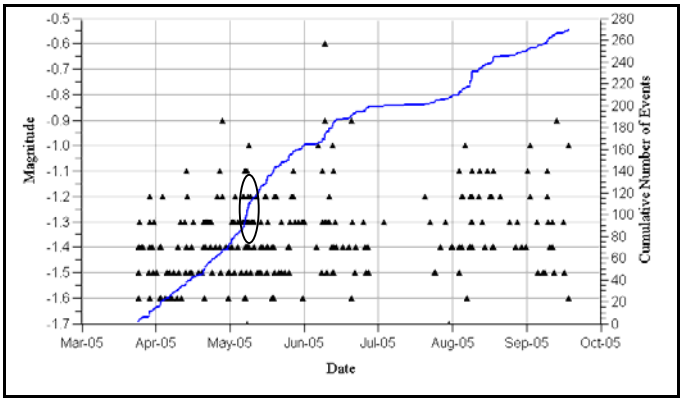

Fig. 8. Moment magnitude vs. time. An Increase in the activity rate associated with heavy rainfalls in May is indicated.

The seismic energy to moment relationship is shown in Fig. 9, with a considerable spread. The linear regression has a slope of 1.8, considerably higher than 1, commonly observed for earthquakes and indicative of a constant stress-drop at the source. A relatively narrow range of source parameters is obtained, leading to an anomalously high b-value of 3.1 for this dataset (Fig. 10). This result suggests that mining induced abutment stresses may be responsible for creating a rock fragmentation very different than the distribution expected for a typical tectonic regime (b = 1).

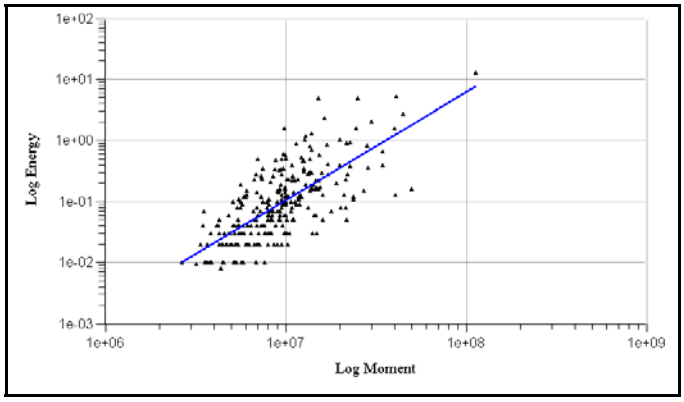

Fig. 9. Energy vs. seismic moment.

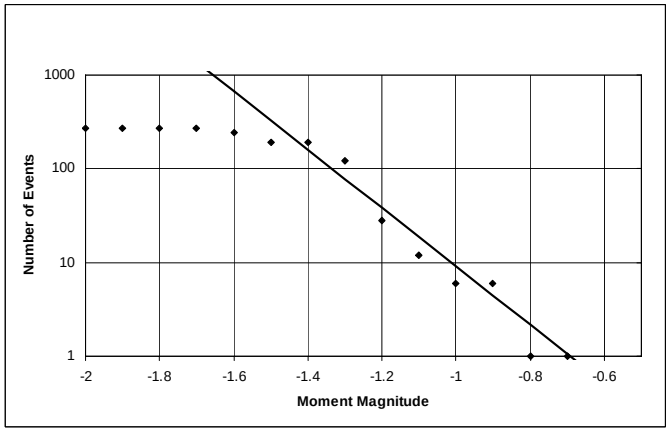

Fig. 10. Frequency-magnitude distribution.

A plot of cumulative E_S / E_P is presented in Fig. 11, where $E_c = 4\pi\rho c R^2 S_{V2c}$. Also shown on this plot are energy ratios for various underground mining operations in Western Australia.

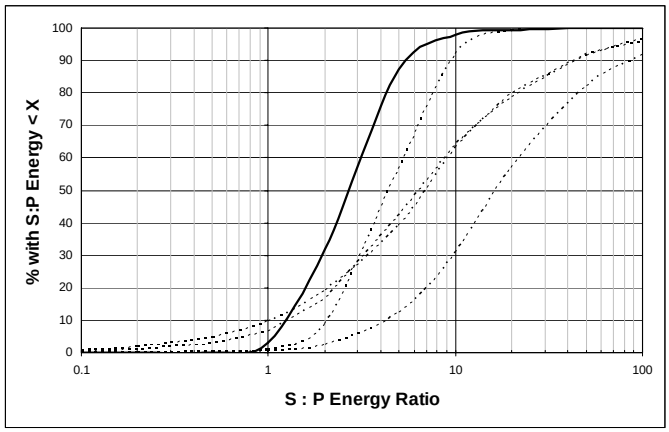

Fig. 11. Cumulative E_S/E_P (solid line) compared to estimates at various underground mines in the region (dotted line).

The analysis indicates that approximately 60% of the events have energy ratios less than 3 and 90% less than 5.5. This implies that the dominant source mechanism is volumetric stress change rather than shear-slip [3], which would suggest either crushing

or dilatational rockmass behaviour. In case of the underground data presented in Fig. 11, three of the four datasets exhibit energy ratios larger than 10 for 35 to 70% of all events, which indicates substantial shear failure components.

All the seismic events located at Site 319 are displayed in Fig. 12. Two clusters are apparent, denoted by A and B. Both clusters are characterized by relatively higher activities, the latter including a considerable percentage of the high magnitude events. However, lack of sufficient data renders individual cluster analysis inconclusive at this stage.

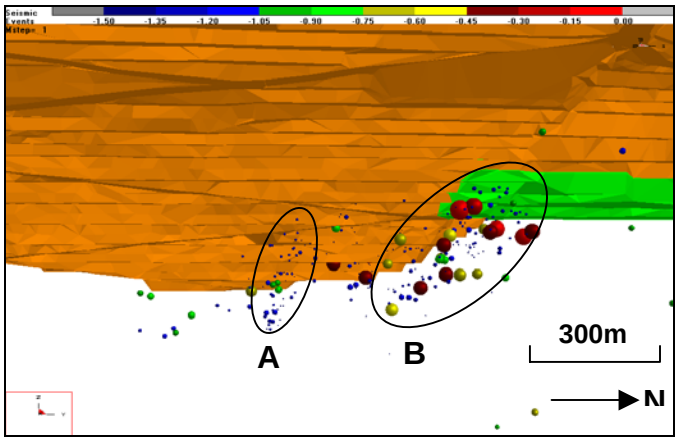

Fig. 12. Seismicity at Site 319 scaled according to moment magnitude. A and B denote apparent clusters.

Cumulative seismic moment (Fig. 13) shows a poor spatial correlation with surface movement (Fig. 14). However when comparing the cumulative moment contours with the void excavated over the same period, high values occur at the intersection between the recently mined void and the previous mining stage. This suggests that the microseismic activity may be associated with the pit geometry and mining induced stresses in the abutment zone.

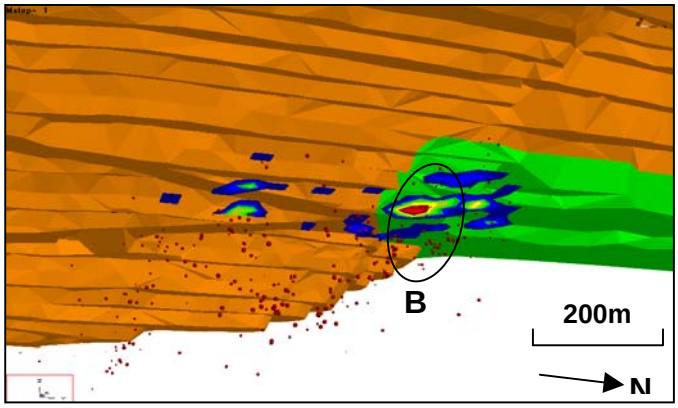

Fig. 13. High cumulative moment estimates (cluster B), are observed at the intersection between a recently excavated void (green) and an existing void (brown).

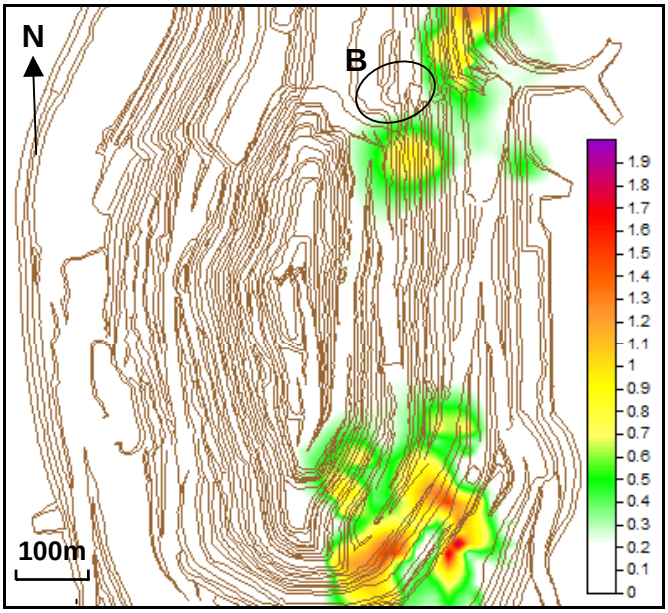

Fig. 14. Surface displacement rate in mm/day during the monitoring period. The position of cluster B is also indicated.

6. FUTURE WORK

At the time of publication, the two additional trial monitoring sites have been installed. Planning is in advanced stages for the expansion of one of the trial site arrays to full size, with a capability to monitor a volume of about 300 x 300 x 300 m.

Based on the results obtained during the trial, the final array is proposed to consist of a combination of twelve uniaxial geophones and four triaxial accelerometers, for a 24-channel system. Uniaxial geophones will provide the network sensitivity required to detect small events, whereas triaxial accelerometers will provide reliable source parameter estimates for the smallest magnitude events. A drilling pattern consisting of a slope-parallel borehole with a vertical borehole on the same section is proposed (Fig. 15).

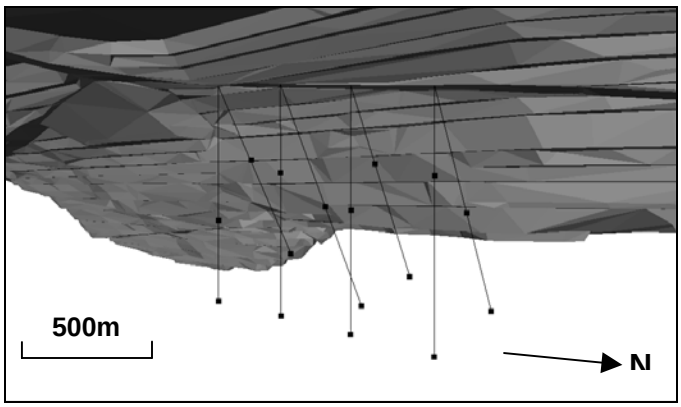

Fig. 15. Conceptual 16-sensor array installed in 8 boreholes.

In conjunction with microseismic monitoring, a rock mechanics numerical modelling study is scheduled. It will make use of stress measurement data collected from borehole cores using acoustic emissions methodology [4], in an attempt to relate the seismicity to mining induced stress and / or deformation.

Mt. Keith's extensive automated displacement (prism) monitoring network will provide the necessary wall movement data to correlate with significant seismic activity. Data from the Ground Probe Slope Stability Radar will also be available to monitor short-term instabilities and correlate them with recorded microseismicity.

ACKNOWLEDGMENTS

This study was funded as part of the project *High Resolution Seismic Monitoring in Open Pit Mines* carried out under the auspices of the Australian Centre for Geomechanics (ACG). Financial support for this project was provided by BHP Billiton (Mt. Keith Nickel Operation), XStrata Zinc (Black Star Pit - Mt. Isa), and Minerals and Energy Research Institute of Western Australia. BHP Billiton (Nickel West) is thanked for the continuous on-site assistance offered by their geotechnical group during the project to date, and for permission to publish this material. The authors would also like to thank Marty Hudyma (ACG) for his initial suggestions and ongoing support.

REFERENCES

1. Lee, M., M. Pascoe, and P. Mikula. 1999. Stress field in Western Australia, a Kambalda-Kalgoorlie case study. In *Proceedings of the Workshop on Mining in High Stress and Seismically Active Conditions*, Australian Centre for Geomechanics, Perth. Section 2, pp. 1-21.

2. Trifu, C-I. and V.Shumila. 2002. Reliability of seismic moment tensor inversions for induced microseismicity at Kidd mine, Ontario. *Pure and Applied Geophysics*, 159, 145-164.

3. Boatwright, J., and J.B. Fletcher. 1984. The partition of radiated energy between P and S waves. *Bull. Seismol. Soc. Am.* 74: 361-376.

4. Villaescusa, E., M. Seto, and G. Baird. 2002. Stress measurements from oriented core. *Int. J. Rock Mec. Min. Sci.* 39: 603-615.